Original Article

Methylation of *PLIN5* is a crucial biomarker and is involved in ovarian cancer development

Yujie Zhao[1#], Dong Xu[2#], Ying Wan[3], Qinghua Xi[1]

[1]Department of Obstetrics and Gynecology, Affiliated Hospital of Nantong University, Nantong 226001, China; [2]Department of Obstetrics and Gynecology, Huai'an First People's Hospital, Huai'an 223001, China; [3]Department of Geratology, Nantong University No. 2 Affiliated Hospital, Nantong 226001, China

Contributions: (I) Conception and design: Y Zhao, Q Xi; (II) Administrative support: Q Xi; (III) Provision of study materials or patients: D Xu, Y Wan; (IV) Collection and assembly of data: Y Zhao, Y Wan; (V) Data analysis and interpretation: D Xu; (VI) Manuscript writing: All authors; (VII) Final approval of manuscript: All authors.

[#]These authors contributed equally to this work.

Correspondence to: Dr. Qinghua Xi. Department of Obstetrics and Gynecology, Affiliated Hospital of Nantong University, No. 20, Xisi Road, Nantong 226001, China. Email: xiqinghuazhaoyujie@163.com; Dr. Ying Wan. Department of Geratology, Nantong University No. 2 Affiliated Hospital, 6 Nantong Haier Lane Road, Nantong 226001, China. Email: wy2064@126.com.

Background: *PLIN5* is abnormally expressed in many forms of tumors, but its activity and methylation status in human ovarian cancer (OC) have yet to be elucidated.

Methods: RNA sequencing data (RNA-seq) were downloaded from The Cancer Genome Atlas (TCGA) and Genotype-Tissue Expression (GTEx) database. Differentially expressed genes (DEGs) were identified, and then *PLIN5* gene was selected for further study. Expression and methylation levels of *PLIN5* were detected by qPCR, western blot, immunohistochemical, and MSP analysis. Moreover, colony formation, transwell, and cell apoptosis assays were employed to explore the abilities of cell proliferation, migration, invasion, and apoptosis, respectively. Furthermore, *PLIN5*'s function on tumorigenesis was determined by in vivo experiments.

Results: We found that *PLIN5* was downregulated in OC tissues by using qPCR, western blot, and immunohistochemical analyses, and MSP also exhibited that *PLIN5* was hypermethylated in OC tissues. The expression level of *PLIN5* could be restored after treatment with 5-Aza-dC. Furthermore, we found that demethylated *PLIN5* could suppress cell proliferation, migration, and invasion of OC, and increase cell apoptosis. Moreover, xenograft experiments showed that demethylated *PLIN5* could suppress tumor growth.

Conclusions: Our findings suggest that the expression level of *PLIN5* is regulated by methylation, and in OC, *PLIN5* can act as a tumor suppressor.

Keywords: Ovarian cancer (OC); *PLIN5*; methylation; 5-Aza

Submitted Mar 04, 2020. Accepted for publication Mar 26, 2020.
doi: 10.21037/tcr-20-1221
View this article at: http://dx.doi.org/10.21037/tcr-20-1221

Introduction

Ovarian cancer (OC), a leading type of malignant tumors in gynecological, and its incidence is increasing globally (1). Despite the progress in surgery, chemotherapy, and radiotherapy, the clinical prognosis of OC remains unsatisfactory, and most OC patients ultimately die of recurrence and metastasis (2). Hence, it is necessary to reveal the potential molecular mechanisms of OC occurrence and metastasis to identify new epigenetic biomarkers for OC therapy.

Both epigenetic and genetic aberrant changes are seen as essential to carcinogenesis (3). DNA methylation is the most characterized epigenetic modification. The methylation of CpG island leads to the inactivation of tumor suppressor

gene transcription, which has become an important part of cancer epigenetic research (4). Therefore, investigation on the changes in DNA methylation in cancer can help to better elucidate the mechanisms of tumor development.

In this study, we used the TCGA and GTEx datasets to screen out *PLIN5* as a hub gene and as a new molecular target in OC. Perilipin 5 (*PLIN5*) is a vital member of the perilipin family, and is especially prominent in oxidative tissues, including in heart, brown adipose, skeletal muscle, and liver tissues (5). *PLIN5* is considered to mediate mitochondrial function and to control the concentration and release of fatty acids to sustain lipid droplet homeostasis (6). Moreover, we explored the expression and degree of methylation of *PLIN5* in OC tissues and analyzed its effects on the proliferation and metastasis of OC cells.

Methods

Gene expression data

RNA sequencing data (RNA-seq) of the OC samples was downloaded from TCGA (7), and RNA-seq of the normal ovarian specimen was collected from the GTEx project (8). The edgeR package was employed to screen out the DEGs with |logFC| >1 and false discovery rate (FDR) <0.05 (9). In all transcriptomic data, we used only protein-related genes. Those protein genes with logFC >1 and FDR <0.05 were deemed as upregulated, and those genes with logFC <–1 and FDR <0.05 were deemed as downregulated.

Function enrichment analyses

Gene Ontology (GO) (10) and KEGG pathway (11) enrichment analyses were applied by the DAVID (12). Besides, GO terms comprised the biological process (BP), cellular component (CC), and molecular function (MF). FDR <0.05 were considered as significant.

Clinical samples and cell culture

This study examined all patients with OC who underwent surgery Affiliated Hospital of Nantong University. And none of the patients received any treatment before the operation, and all patients had given their informed written consent. Fresh tissue samples were immediately stored at –80 ℃. Moreover, the study protocol has been approved by the Affiliated Hospital of Nantong University.

The SKOV3, HO8910, OV90, and HOSE cell lines were cultured at 37 ℃ and 5% CO_2 in DMEM or RPMI-1640 medium (Gibco) with 10% fetal bovine serum (FBS) (Invitrogen). Transfection was applied by using liposome Lipofectamine 3000 (Invitrogen). Transfected cells were harvested and used for further experimental research.

Quantitative real-time polymerase chain reaction (qPCR)

Total RNA was extracted by TRIzol (Invitrogen). Then, cDNA was reversely transcribed with a SuperScript First-Strand Synthesis System (Invitrogen). qPCR reactions were applied by using the SYBR Green PCR Master Mix (Roche). Primers: *PLIN5* forward, 5'-TGCCCATGACGGAGGAAGA-3', *PLIN5* reverse, 5'-GAGCCGAGGCGCACAAA-3'. The relative expression levels were normalized by the Ct value of GAPDH using a $2^{-\Delta\Delta Ct}$ method.

Western blot analysis

The lysates were extracted, and total protein was isolated by 10% SDS/PAGE gels and transferred to nitrocellulose membranes. The membranes were blocked in 5% fat-free milk for 1 h at room temperature, and then incubated with the primary antibodies overnight at 4 ℃: rabbit polyclonal anti-*PLIN5* (Abcam; 1:1,000; cat. no. ab222811), and mouse monoclonal anti-β-actin (1:2,500). After washing three times with Tris-buffered saline (TBS) containing 0.1% Tween-20, the membrane was incubated secondary antibody, anti-rabbit IgG conjugated IRDye800 (1:5,000, Rockland Gilbertsville, CA) for 2 h at room temperature. At last, the protein bands were tested using the ECL Plus kit (ZSbio).

Immunohistochemical staining

Paraffin-embedded tissues were analyzed by using tissue microarray (TMA) analysis. Tissue sections were dewaxed and rehydrated in graded ethanol. Then, antigen retrieval was achieved by boiling sections in EDTA buffer (pH 6.0) for 3 min. The endogenous peroxidase activity was quenched with 3% hydrogen peroxide for 30 min, and the TMA slides were stained overnight with a rabbit polyclonal anti-*PLIN5* antibody (Abcam) at 4 ℃ The goat anti-rabbit secondary antibody (Sigma) combined with horseradish peroxidase was incubated at 37 ℃ for 30 min. Then, slides were treated with horseradish peroxidase and 3,3-diaminobenzidine chromogen solution, and then counterstained with hematoxylin. The semiquantitative

scoring system was based on both the staining intensity and the percentage of cells at that intensity. According to the pathological score, the staining intensity was divided into 0 (–, no staining), 1 (+, weak staining), 2 (++, moderate staining), or 3 (+++, intense staining). The percentage of stained cells was evaluated and multiplied by the intensity score to generate an intensity percentage score. Finally, the staining score was the sum of the four intensity percentage scores, ranging from 0 (no staining) to 300 (100% of cells with +++ staining intensity).

Methylation-specific PCR (MSP)

Genomic DNA was extracted by using a DNeasy tissue kit (Qiagen). The sodium bisulfite reaction was applied to 5 μg genomic DNA using the EpiTect Bisulfite Kit (Qiagen). The primers of MSP were as follows: (M): forward, 5'-GATGATAGGTGGTTAAATTTGGTTC-3' and reverse, 5'-TTAAACTAACCCAATACCCTACG AT-3'; and unmethylated-specific primers (U): forward, 5'-ATGATAGGTGGTTAAATTTGGTTTG-3' and reverse, 5'-CCTTAAACTAACCCAATACCCTACAA-3'.

Demethylation with 5-aza-2'-deoxycytidine (5-Aza-dC) treatment

Cells were seeded into six-well plates at a concentration of 1×10^6 cells per well and cultured at room temperature for 24 h. Next, cells were processed by using 1 μM of 5-Aza-dC (13) (Sigma) for 72 h. And the culture medium was changed every day.

Colony formation assay

Cells were seeded into six-well plates in complete medium and cultured for 2 weeks. Cells were fixed with 100% methanol for 10 min and stained with 0.5% crystal violet for 20 min at room temperature, and the number of colonies (>50 cells) was calculated under an optical microscope.

Cell apoptosis

Briefly, after 72 h of transfection, cells were harvested and resuspended in the Annexin-binding buffer at a concentration of 1×10^6 cells/mL, then stained in the dark with Annexin V-FITC and PI for 15 min at room temperature, and then analyzed with the FACSCalibur flow cytometer.

Transwell assay

For the migration assays, cells (1×10^5 cells/well) were added to the upper Transwell chambers (Corning, 8-μm pore size). Cells were cultured in serum-free medium, and 10% FBS serum medium was used as the chemical attractant in the lower chambers. For the invasion assays, cells were plated on the upper side of the chambers with Matrigel (BD Biosciences) and incubated in the medium. A medium containing 10% FBS was injected into the lower chamber to attract cells. After incubation in a humidified atmosphere with 5% CO_2 at room temperature for 24 h, cells that did not migrate or invade to the pores with cotton wool were removed. Cells on the lower membrane were fixed with 100% methanol for 10 min and stained with 0.2% crystal violet for 20 min at room temperature. Finally, images of the inserts were taken under an inverted microscope (Olympus), and the migrated and invaded cells were calculated in five randomly fields.

Xenograft experiments

Firstly, BALB/c nude mice were applied for tumorigenesis experiments. Then, the mice were subcutaneously injected or inoculated with 1×10^6 cells/100 μL per side, 7 per group). Tumor length (L) and width (W) were assessed weekly. The calculation formula of tumor volume was as follows: tumor volume = width^2 × length/2. After about 4 weeks, the mice were sacrificed and the peritoneal metastatic nodules were measured.

Statistical analysis

All experiments were performed in triplicate. SPSS 21.0 statistical software (SPSS, IL, USA) was performed for the statistical analysis. A paired *t*-test was employed to analyze the statistical significance of the differences between the two groups. A one-way analysis of variance (ANOVA) test was employed to analyze the statistical significance of the differences between the three groups. $P<0.05$ was determined as statistically significant.

Results

Identification of DEGs in OC and enrichment analyses

To identify the expression pattern of genes, we screened DEGs from the RNA-Seq data of the OC cases in TCGA and normal cases from the GTEx database. The heatmaps

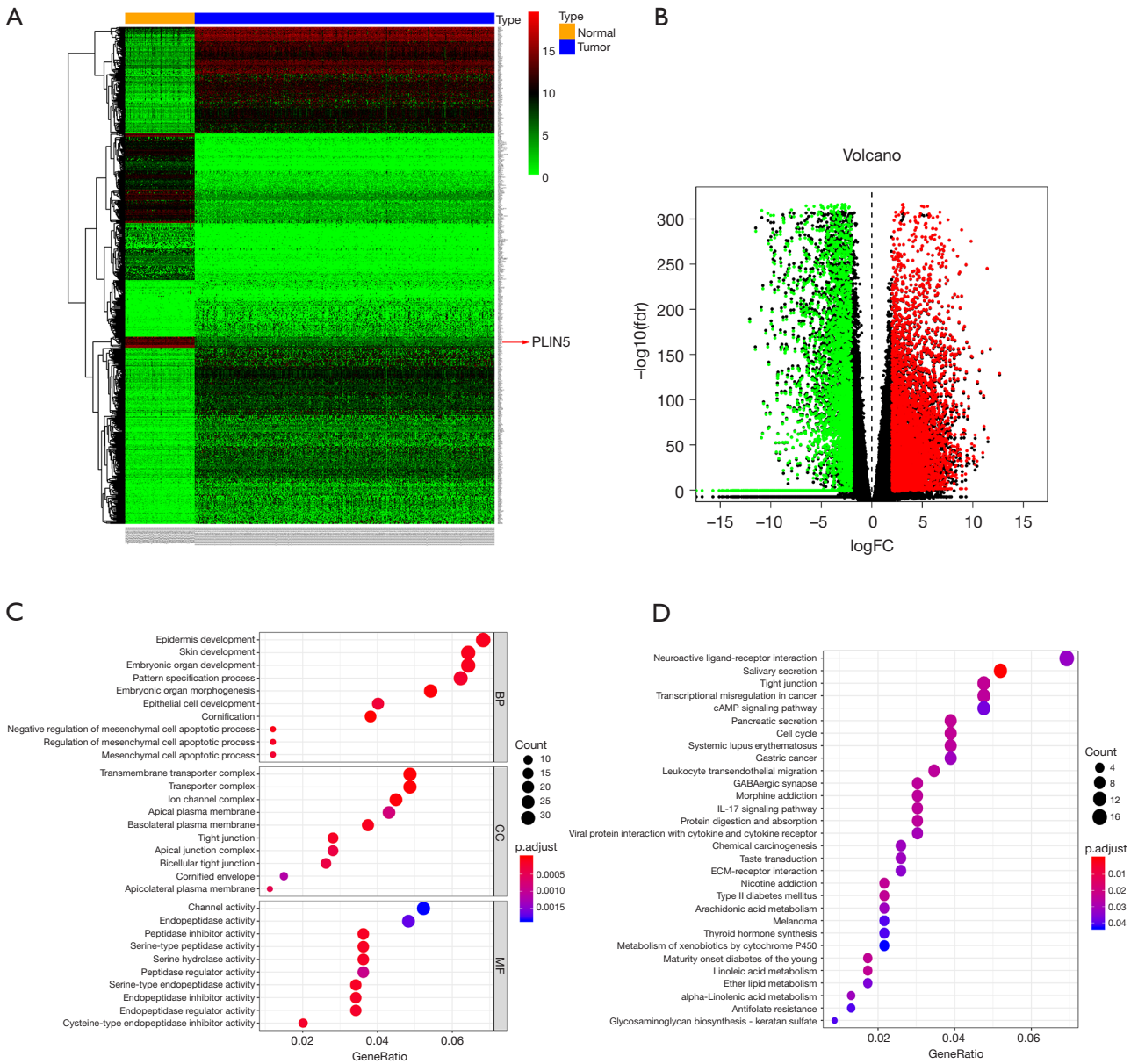

Figure 1 Hierarchical cluster analysis and functional enrichment analysis. (A,B) Heatmaps and volcano plot of DEGs between OC and normal tissues in TCGA and GTEx datasets; (C,D) GO and KEGG pathway analysis of the DEGs in OC. DEGs, differentially expressed genes; OC, ovarian cancer; TCGA, The Cancer Genome Atlas; GTEx, Genotype-Tissue Expression; GO, Gene Ontology.

exhibited the upregulated and downregulated DEGs in datasets (*Figure 1A*). Also, the volcano plot showed 634 DEGs, including 446 upregulated genes and 188 downregulated genes (*Figure 1B*). To further investigate the biological effects of these DEGs in OC, we completed an enrichment analysis. The results of GO analysis revealed that these DEGs were most dramatically enriched in cornification (BP), transmembrane transporter complex (CC), and peptidase inhibitor activity (MF). Moreover, KEGG pathway analysis presented that these DEGs were primarily enriched in salivary secretion, pancreatic secretion, among other processes (*Figure 1C,D*).

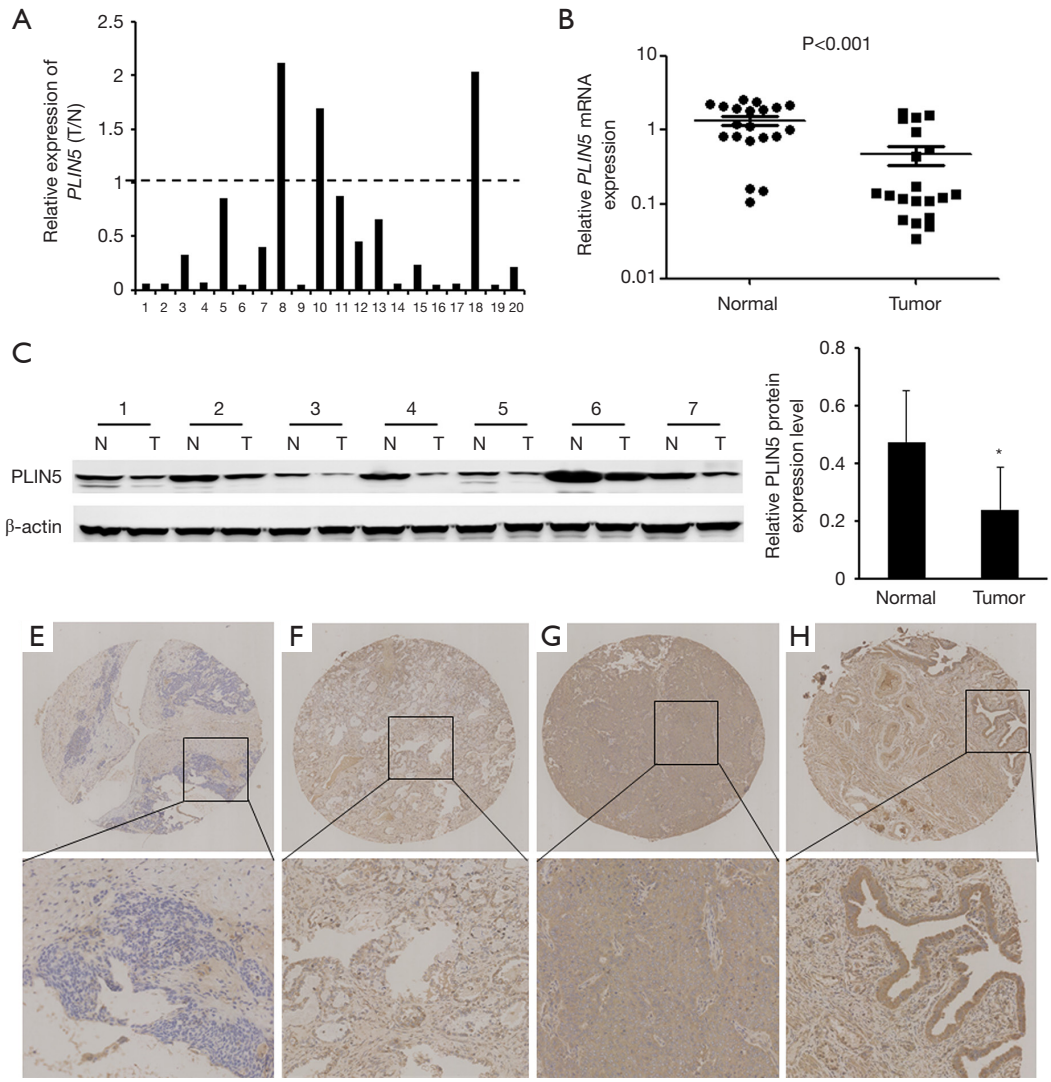

Figure 2 Expression levels of *PLIN5* in ovarian cancer. (A) qPCR analysis indicated that *PLIN5* expression was downregulated in 20 OC tissues. (B) The downregulation of *PLIN5* was statistically significant compared to normal tissues. (C) Western blot analysis of representative paired samples of OC (T) and their matched adjacent normal tissues (N). (D) Relative average PLIN5 protein expression levels were significantly downregulated in OC tissues compared with the corresponding adjacent normal tissues (*, P<0.05). Representative patterns of *PLIN5* expression in ovarian tissues were present by immunohistochemical analysis. (E) OC samples weakly positively stained with a staining index marked as +. (F) OC samples moderately positively stained with a staining index marked as ++. (G) OC samples strongly positively stained with a staining index marked as +++. (H) Normal ovarian samples strongly positively stained with a staining index marked as +++. Original magnification, ×40 or ×200. OC, ovarian cancer.

Expression and methylation levels of PLIN5 in OC tissues and cells

The levels of *PLIN5* expression was examined with qPCR analysis, which indicated that *PLIN5* expression were markedly lower in OC tissues compared to the normal tissues (*Figure 2A,B*). The results were confirmed to examine the PLIN5 protein level by western blot in 20 random pairs of OC and matched adjacent normal tissues. Then, the representative results of the western blot in 7 cases were exhibited in *Figure 2C*. The above results demonstrated that the PLIN5 protein level was reduced in the tumor samples compared with matched adjacent normal

Table 1 Correlation of clinicopathologic characteristics with *PLIN5* expression

Characteristics	Total (n=57)	*PLIN5* expression		P value
		Low (n=32)	High (n=25)	
Age (years)				0.366
≤50	22	14	8	
>50	35	18	17	
Tumor size (cm)				0.492
≤5	20	10	10	
>5	37	22	15	
Location				0.845
Right	13	8	5	
Left	12	6	6	
Bilateral	32	18	14	
Histology				0.130
Serous adenocarcinoma	40	19	21	
Clear cell carcinoma	8	6	2	
Mucinous adenocarcinoma	9	7	2	
FIGO stage				0.376
I	8	6	2	
II	13	8	5	
III	32	15	17	
IV	4	3	1	
Lymph node metastasis				0.446
Yes	5	2	3	
No	52	30	22	
Distant metastasis				0.010*
M0	14	12	2	
M1	43	20	23	

*, P<0.05 was considered significant.

tissues (*Figure 2D*; P<0.05). These above data indicated that *PLIN5* was downregulated in OC tissues. Furthermore, TMA-based immunohistochemical analysis was performed in 57 OC tissues and 12 normal ovarian tissues. The representative results were shown in *Figure 2E,F,G,H*. The positive staining was mainly localized in the cytoplasm of tumor cells. *PLIN5* showed strongly positive staining in 12 normal ovarian tissues, and 57 OC tissues were positively stained for *PLIN5*, 32 cases showed low expression of *PLIN5*, and 25 cases showed high expressions of *PLIN5*. Moreover, the correlation between the expression of *PLIN5* and the clinicopathologic factors of these OC patients are summarized in *Table 1*. The data showed that low *PLIN5* expression was observably related to distant metastasis (P=0.010).

Previous studies have shown that the methylation status of the CpG islands may closely correlated with the regulation of gene expression (14). Therefore, we used

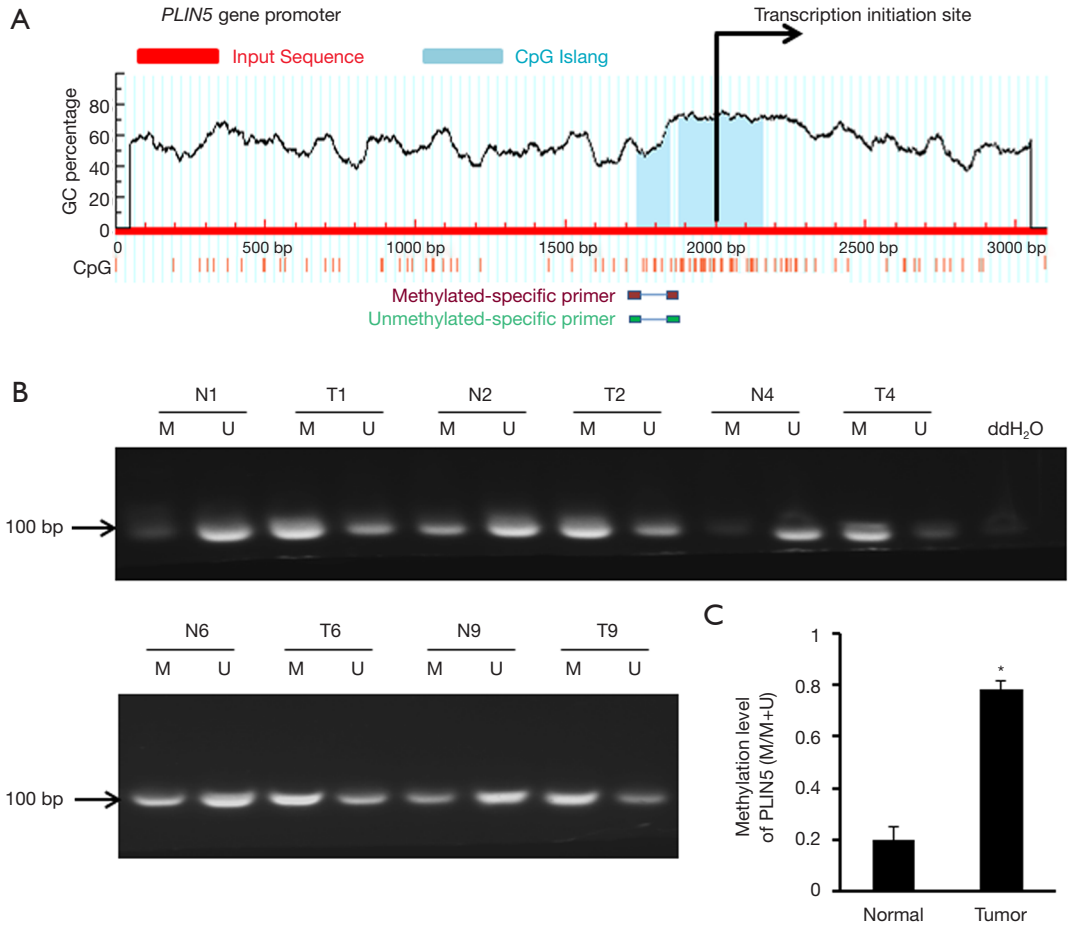

Figure 3 *PLIN5* expression is regulated by promoter region methylation in ovarian cancer. (A) MethPrimer analysis showed that the scheme of the location of the CpG islands is located in the region of the *PLIN5* gene promoter; (B) representative MSP results indicated the *PLIN5* degree of methylation in normal tissues and tumor tissues; (C) compared with that of the normal tissues, the *PLIN5* methylation degree in tumor tissues was increased. *, P<0.05.

MethPrimer software to search for the status of CpG islands in the promoter region of *PLIN5* and found significant CpG islands (*Figure 3A*). MSP analysis was employed to detect the methylation status of *PLIN5* in OC and normal tissues. And the methylation levels of *PLIN5* in cancer tissues were distinctly increased compared with normal tissues (*Figure 3B,C*). Next, *PLIN5* expression in SKOV3, HO8910, and OV90 cell lines was measured by western blot and qPCR analyses. The results exhibited that the protein and mRNA levels of *PLIN5* were decreased in OC cell lines, compared with HOSE cell lines (*Figure 4A,B*). Furthermore, the methylation levels of *PLIN5* in HO8910, SKOV3, and OV90 were elevated compared with that of the HOSE cell line (*Figure 4C*, P<0.05).

Restored PLIN5 expression inhibited the progression of OC cells

Firstly, the number of clones was remarkably lower in the *PLIN5* overexpression group and the 5-Aza group than in the NC and sh-*PLIN5* + 5-Aza groups by using colony formation assay (*Figure 5A*). The apoptosis rate of the OV90 cells transfected with *PLIN5* or 5-Aza was dramatically increased compared with the NC and sh-*PLIN5* + 5-Aza groups (*Figure 5B*, P<0.05). In addition, transwell assays exhibited that the ability of cell migration and invasion decreased significantly in the *PLIN5* and 5-Aza groups relative to the NC and sh-*PLIN5* + 5-Aza groups (*Figure 6A,B*).

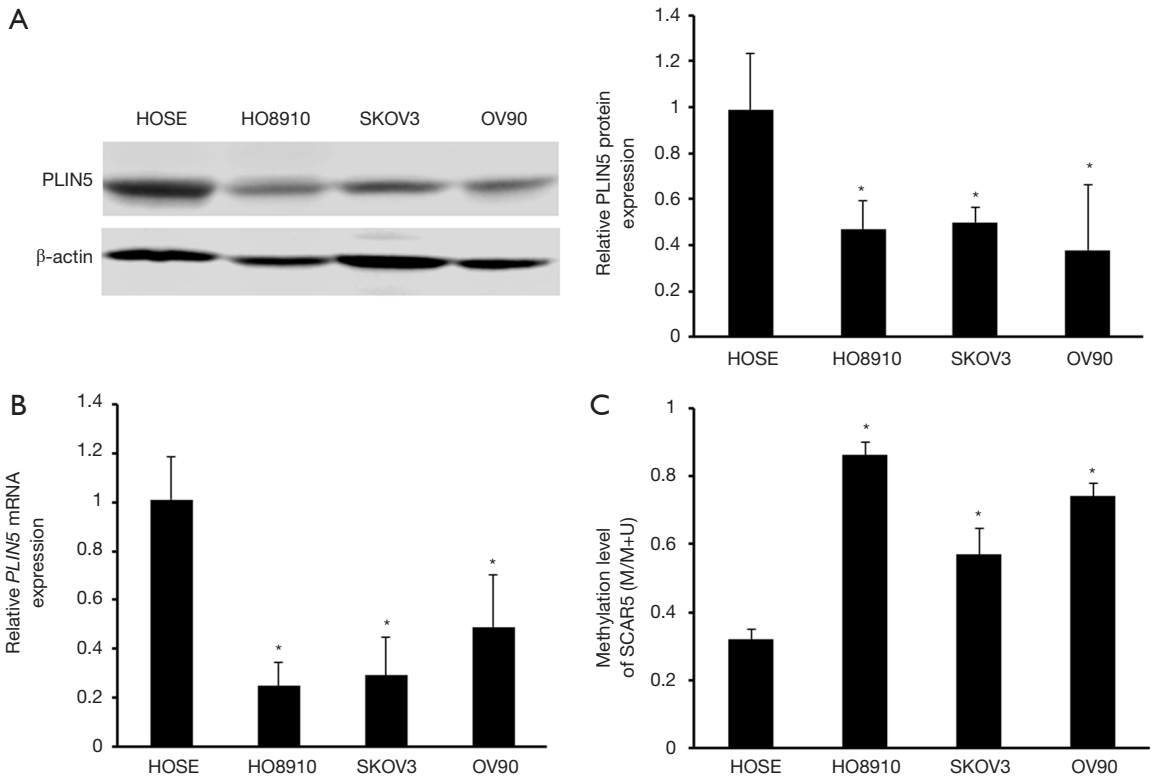

Figure 4 Expression and methylation status of *PLIN5* in ovarian cancer cells. (A) The protein expression levels of *PLIN5* were detected by western blot in OC cell lines. Western blot analysis indicated the PLIN5 protein expression levels in SKOV3, OV90, and HO8910 cell lines compared with the HOSE cell line. *, P<0.05. (B) qPCR analysis indicated the *PLIN5* mRNA expression levels in SKOV3, OV90, and HO8910 cell lines compared with the HOSE cell line. *, P<0.05. (C) The methylation levels of *PLIN5* in HO8910, SKOV3, and OV90 were dramatically increased compared with that of the HOSE cell line. *, P<0.05. OC, ovarian cancer.

To further assess the effects of *PLIN5* on the proliferation of OC cells *in vivo*, we observed tumor weight and volume after transfected OV90 cells with *PLIN5* overexpression plasmid. The results showed that tumor weight and volume in the *PLIN5* group were lower than those in the NC group (*Figure 7*, P<0.05). All the above results suggested that *PLIN5* may serve as a tumor suppressor gene, which could suppress cell proliferation, migration, and invasion of OC while promoting apoptosis.

Discussion

Nowadays, the poor prognosis of OC patients is attributed primarily to the challenging diagnosis and likelihood of early metastasis. These two factors highlight the importance of revealing the molecular mechanisms of an OC metastasis. To improve the prognosis of OC patients, new biomarkers and therapeutic targets are urgently needed (15). In the current study, the DEGs in OC patients were analyzed by using data from the TCGA and GTEx databases, and we found that *PLIN5* was significantly downregulated in the tumor samples. Moreover, we identified a significant CpG island in the promoter region of *PLIN5*. Therefore, *PLIN5* was selected for further study.

PLIN5 is reported to be specifically expressed in fatty acid oxidized tissues, such as adipose, heart, liver, and muscle tissue (16). The preliminary research in *PLIN5* focused on its function in the heart because of its high oxidative capacity, and most of these studies have pointed out the protective effect of *PLIN5* against hepatic lipotoxicity in the liver (17). Interestingly, *PLIN5* overexpression was found to enhance cellular lipid droplet accumulation, while knockdown of *PLIN5* promoted fatty acid oxidation metabolism (18). Another recent study

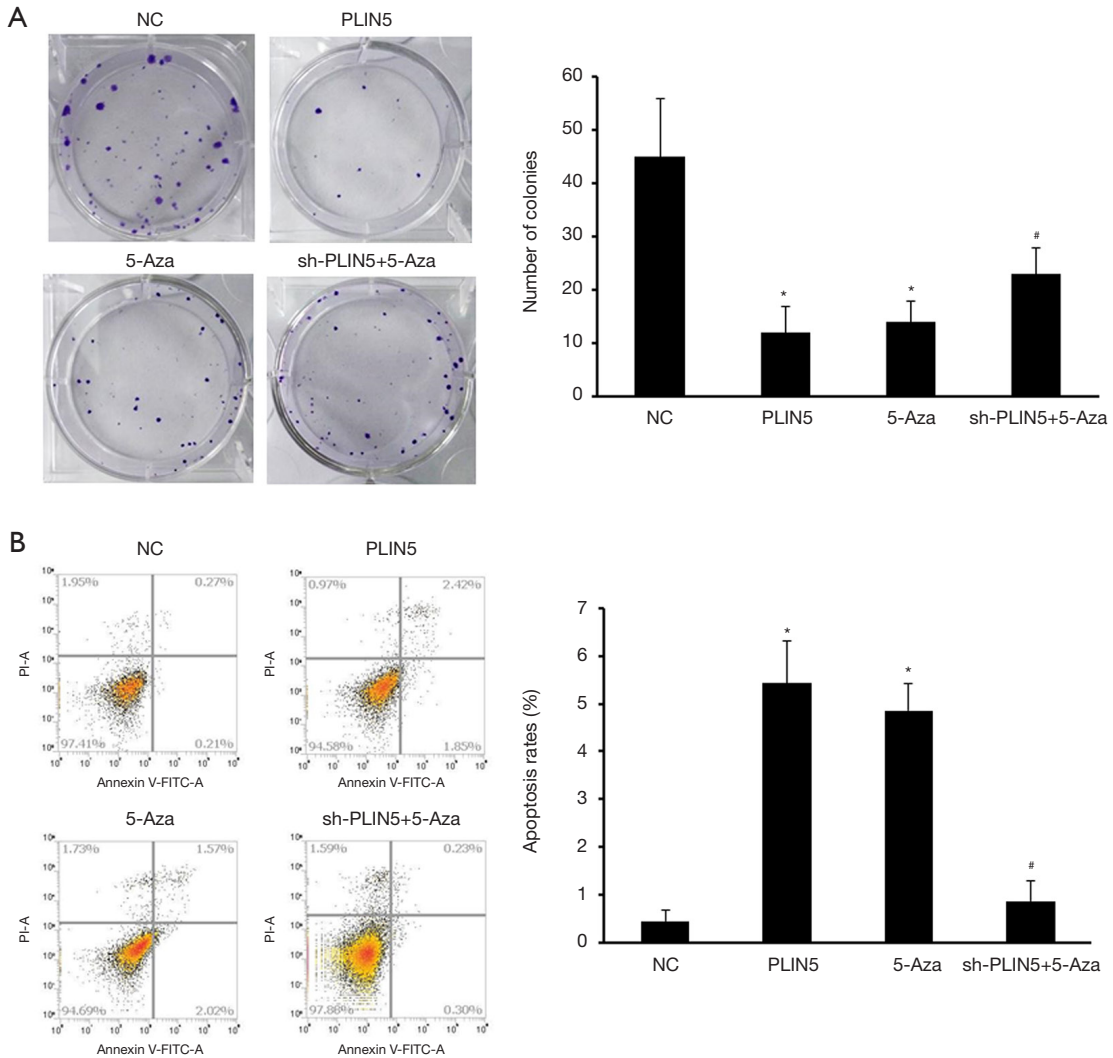

Figure 5 Restored expression of *PLIN5* inhibits cell proliferation. (A) The number of clones was decreased in the *PLIN5*-overexpressing group and the 5-Aza group compared with the NC group. *, P<0.05, compared with the NC group; #, P<0.05, compared with the 5-Aza group. Original magnification, ×100. (B) The apoptosis rate of SKOV3 cells transfected with *PLIN5* or 5-Aza dramatically increased compared with the NC group. *, P<0.05, compared with the NC group; #, P<0.05, compared with the 5-Aza group.

has reported that *PLIN5* exists in renal cell carcinoma, rhabdomyosarcoma, liposarcoma (16), and hepatocellular carcinoma (19). Thus, we believe that *PLIN5* could regulate reactive oxygen species (ROS) levels, and lipid content and lipolysis of cells, which could affect the development of a tumor. Furthermore, the down-regulation of *PLIN5* may induce tumorigenesis (20). In this study, to further verify the *PLIN5* expression level and methylation degree, western blot, qPCR, immunohistochemical and MSP analysis were employed and showed that *PLIN5* was hypermethylated and *PLIN5* expression was reduced in OC tissues.

Our study also explored the biological functions of the *PLIN5* gene in the genesis and development of OC. The results of the experiments revealed that *PLIN5* overexpression could dramatically suppress cell proliferation, migration, and invasion, and promote apoptosis in vitro. Additionally, it is suggested that the changes in DNA methylation may be of significance to the diagnosis, prognosis, and treatment of OC (21). Studies have shown that DNA hypermethylation silences

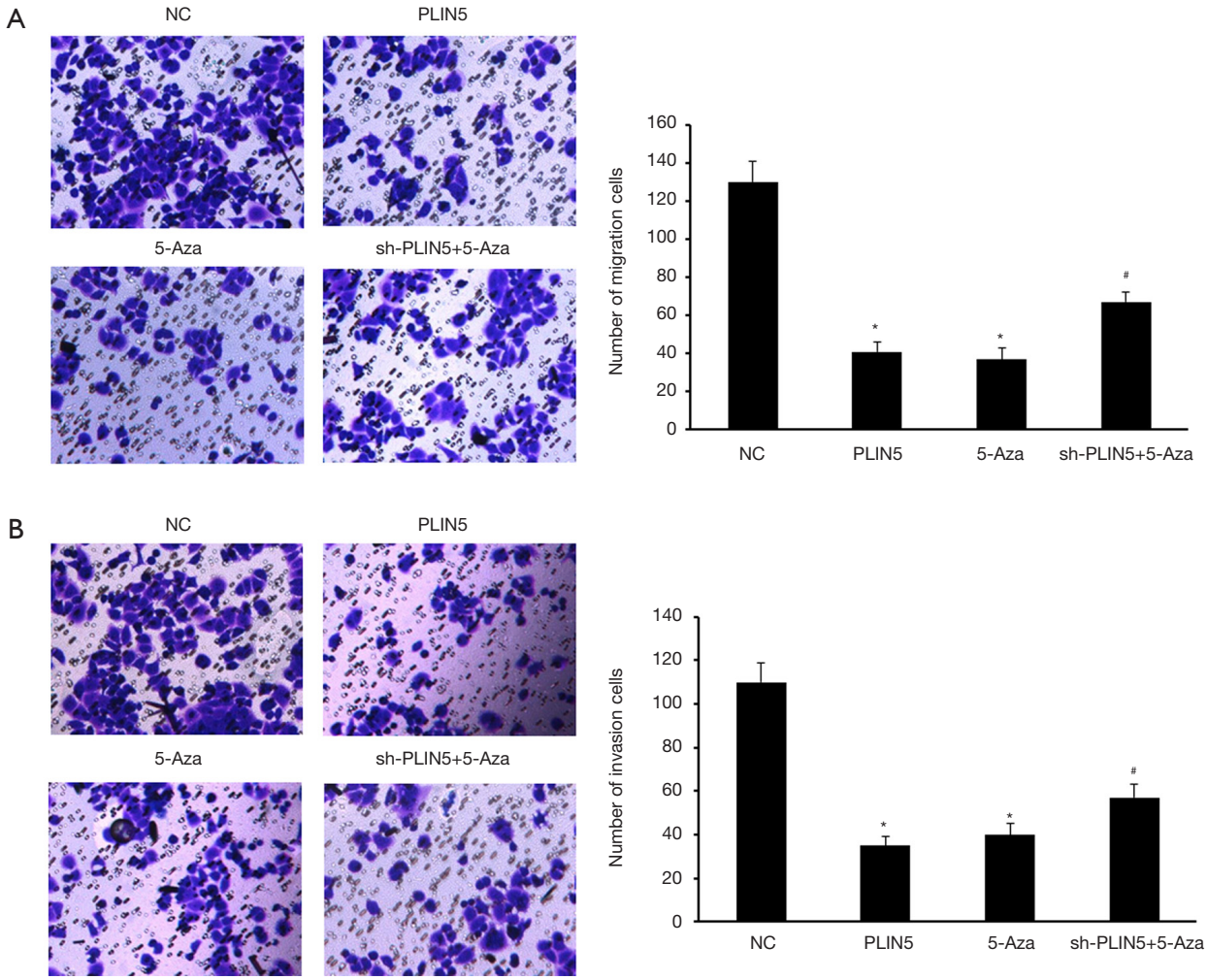

Figure 6 Restored expression of *PLIN5* inhibits cell migration and invasion. (A,B) Transwell assays revealed that the abilities of cell migration and invasion were remarkedly reduced in the *PLIN5* and 5-Aza groups compared to the control group. *, P<0.05, compared with the NC group; #, P<0.05, compared with the 5-Aza group. Representative photos of stained cells are shown with the original magnification of ×100.

the genes needed for tumor development (22). Moreover, DNA methylation is a reversible epigenetic modification. 5-Aza, a DNA methyltransferase inhibitor, can reverse the hypermethylation in the promoter region, re-express tumor-related genes, and inhibit tumor cell growth (23). Therefore, we added the 5-Aza + sh-*PLIN5* treatment group to further exhibit a significant effect on cell proliferation, apoptosis, migration, and invasion of OC after DNA methylation inhibition was significantly improved compared with the *PLIN5* overexpression and 5-Aza treatment groups.

Conclusions

To conclude, we found that the promoter region methylation regulates the expression of *PLIN5* in OC. Also, we showed that *PLIN5* expression level was downregulated in OC, and methylation of *PLIN5* is associated with OC metastasis. At last, it is suggested that the *PLIN5* may be a

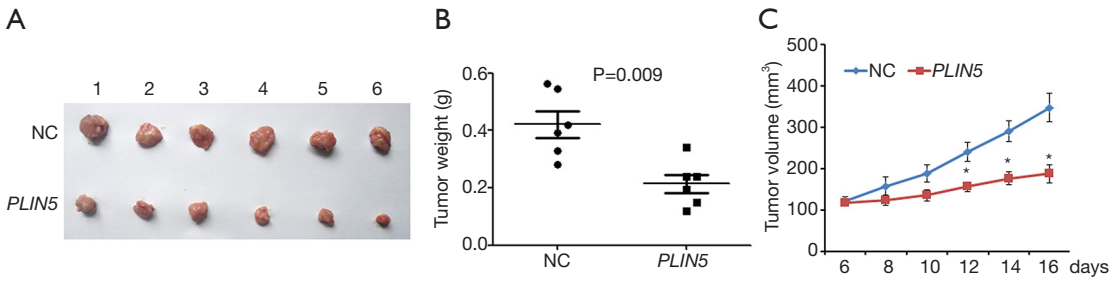

Figure 7 Overexpression of *PLIN5 in vivo* inhibits tumor growth. (A,B,C) Tumor xenograft results showed that tumor weight and volume were reduced in the *PLIN5* group compared with the control group. *, P<0.05.

potential therapeutic target for OC.

Acknowledgments

Funding: This work was supported by grants from the Nantong Science and Technology Project (MS32017009).

Footnote

Conflicts of Interest: All authors have completed the ICMJE uniform disclosure form (available at http://dx.doi.org/10.21037/tcr-20-1221). The authors have no conflicts of interest to declare.

Ethical Statement: The authors are accountable for all aspects of the work in ensuring that questions related to the accuracy or integrity of any part of the work are appropriately investigated and resolved. This study was approved by the Ethics Committee of the Affiliated Hospital of Nantong University (2013-066). Informed consent was provided by all participants.

References

1. Jayson GC. Ovarian cancer. Lancet 2014;384:1376-88.
2. Karnezis AN, Cho KR, Gilks CB, et al. The disparate origins of ovarian cancers: pathogenesis and prevention strategies. Nat Rev Cancer 2017;17:65-74.
3. Kelly AD, Issa JPJ. The promise of epigenetic therapy: reprogramming the cancer epigenome. Curr Opin Genet Dev 2017;42:68-77.
4. Carrió E, Suelves M. DNA methylation dynamics in muscle development and disease. Front Aging Neurosci 2015;7:19.
5. Dalen KT, Dahl T, Holter E, et al. LSDP5 is a PAT protein specifically expressed in fatty acid oxidizing tissues. Biochim Biophys Acta 2007;1771:210-27.
6. Mason RR, Watt MJ. Unraveling the roles of PLIN5: linking cell biology to physiology. Trends Endocrinol Metab 2015;26:144-52.
7. Zhu Y, Qiu P, Ji Y. TCGA-Assembler: open-source software for retrieving and processing TCGA data. Nat Methods 2014;11:599-600.
8. GTEx Consortium. The Genotype-Tissue Expression (GTEx) project. Nat Genet 2013;45:580-5.
9. Sun J, Nishiyama T, Shimizu K, et al. TCC: an R package for comparing tag count data with r obust normalization strategies. BMC Bioinformatics 2013;14:219.
10. Liu W, Liu J, Rajapakse JC. Gene Ontology Enrichment Improves Performances of Functional Similarity of Genes. Sci Rep 2018;14;8:12100.
11. Altman T, Travers M, Kothari A, et al. A systematic comparison of the MetaCyc and KEGG pathway databases. BMC Bioinformatics 2013;14:112.
12. Dennis G, Sherman BT, Hosack DA, et al. DAVID: Database for Annotation, visualization, and Integrated Discovery. Genome Biol 2003;4:P3.
13. Xing XQ, Li B, Xu SL, et al. 5-Aza-2'-deoxycytidine, a DNA methylation inhibitor, attenuates hypoxic pulmonary hypertension via demethylation of the PTEN promoter.

Eur J Pharmacol 2019;855:227-34.
14. Gao D, Herman JG, Guo M. The clinical value of aberrant epigenetic changes of DNA damage repair genes in human cancer. Oncotarget 2016;7:37331-46.
15. van den Brand D, Mertens V, Massuger LFAG, et al. siRNA in ovarian cancer - Delivery strategies and targets for therapy. J Control Release 2018;283:45-58.
16. Hashani M, Witzel HR, Pawella LM, et al. Widespread expression of perilipin 5 in normal human tissues and in diseases is restricted to distinct lipid droplet subpopulations. Cell Tissue Res 2018;374:121-36.
17. Wang C, Zhao Y, Gao X, et al. Perilipin 5 improves hepatic lipotoxicity by inhibiting lipolysis. Hepatology 2015;61:870-82.
18. Li H, Song Y, Zhang LJ, et al. LSDP5 Enhances Triglyceride Storage in Hepatocytes by Influencing Lipolysis and Fatty Acid β-Oxidation of Lipid Droplets. PLoS One 2012;7:e36712.
19. Zhu Y, Zhang X, Zhang L, et al. Perilipin5 protects against lipotoxicity and alleviates endoplasmic reticulum stress in pancreatic β-cells. Nutr Metab (Lond) 2019;16:50.
20. Tan Y, Jin Y, Wang Q, et al. Perilipin 5 Protects against Cellular Oxidative Stress by Enhancing Mitochondrial Function in HepG2 Cells. Cells 2019. doi: 10.3390/cells8101241.
21. Chen P, Huhtinen K, Kaipio K, et al. Identification of Prognostic Groups in High-Grade Serous Ovarian Cancer Treated with Platinum-Taxane Chemotherapy. Cancer Res 2015;75:2987-98.
22. Lee ST, Wiemels JL. Genome-wide CpG island methylation and intergenic demethylation propensities vary among different tumor sites. Nucleic Acids Res 2016;44:1105-17.
23. Seelan RS, Mukhopadhyay P, Pisano MM and Greene RM. Effects of 5-Aza-2'-deoxycytidine (decitabine) on gene expression. Drug Metab Rev 2018;50:193-207.

Cite this article as: Zhao Y, Xu D, Wan Y, Xi Q. Methylation of *PLIN5* is a crucial biomarker and is involved in ovarian cancer development. Transl Cancer Res 2020;9(4):2919-2930. doi: 10.21037/tcr-20-1221

